

Self-Consistent-Field Study of the Alignment by an Electric Field of a Cylindrical Phase of Block Copolymer

Chin-Yet Lin and M. Schick

*Department of Physics, University of Washington,
Box 351560, Seattle, WA 98195-1560 U. S. A.*

(Dated: April 10, 2006)

Abstract

Self-Consistent Field Theory is applied to a film of cylindrical-forming block copolymer subject to a surface field which tends to align the cylinders parallel to electrical plates, and to an external electric field tending to align them perpendicular to the plates. The Maxwell equations and self-consistent field equations are solved exactly, numerically, in real space. By comparing the free energies of different configurations, we show that for weak surface fields, the phase of cylinders parallel to the plates makes a direct transition to a phase in which the cylinders are aligned with the field throughout the sample. For stronger surface fields, there is an intermediate phase in which cylinders in the interior of the film, aligned with the field, terminate near the plates. For surface fields which favor the minority block, there is a boundary layer of hexagonal symmetry at the plates in which the monomers favored by the surface field occupy a larger area than they would if the cylinders extended to the surface.

I. INTRODUCTION

With their ability to self-assemble, block copolymers are a natural choice of material to be utilized in the fabrication of devices incorporating periodic arrays^{1,2,3,4}. A major difficulty with the process, however, is that the system rarely forms a single domain of such an array, so a desirable long-range order is absent. Furthermore, preferential interactions between the blocks and substrate can cause the array to be aligned in a direction other than the one desired for use. Alignment of domains can be obtained in several ways, of which the one of interest to us is the use of an electric field^{4,5}. This takes advantage of the fact that the two blocks in general have different dielectric constants, so that it is favorable for the array to align itself such that there is as little induced polarization charge as possible⁶. For lamellar- and cylinder-forming diblocks, this means that a sufficiently strong field will align the array with lamellae or cylinders oriented with their long symmetry axis parallel to the applied field, perpendicular to the electric plates.

If one assumes that the system, in zero external electric field, is characterized by layers of cylinders lying parallel to the substrate and, in large external fields, is characterized by all cylinders oriented perpendicular to the field, then one would like to know both the equilibrium morphology at intermediate field strengths and the phase diagram of the system. Two possibilities were suggested by Thurn-Albrecht et al.⁴. In the first, the electric field has essentially little effect on the arrangement of parallel cylinders up to the field strength at which the perpendicular morphology becomes the globally stable phase. If this situation obtains, one expects that the difference in electrostatic energies of the two configurations would be $E_c^2 \mathcal{A} d_0$, with \mathcal{A} the area of each plate, and d_0 the distance between plates. Hence a first-order transition would take place at a critical electric field, E_c , such that $E_c \propto d_0^{-1/2}$. In the second scenario, an intermediate phase is formed, one in which the surface field is sufficiently strong that a boundary layer near the plates has a different morphology than in the rest of the film. As Thurn-Albrecht et al. reported observing cylinders both in parallel and perpendicular orientations *over a range of field strengths*, the implication was that while the cylinders were oriented perpendicular to the substrate in most of the film, the boundary layer might consist of cylinders oriented parallel to the surface. The difference in electrostatic energies between the perpendicular phase and this intermediate phase is, then, not $E_c^2 \mathcal{A} d_0$, but $E_c^2 \mathcal{A} t$, where t is a length characteristic of the thickness of the boundary

layer. Presumably it depends only weakly on the film thickness, d_0 . Thus one expects that E_c also varies only weakly with thickness for thick films. Thurn-Albrecht et al.⁴ did indeed find that the critical electric field, beyond which only the perpendicular phase was observed, was relatively constant for large film thicknesses.

The existence of an intermediate phase is a consequence of the competition between the surface fields, which prefer a phase in which the cylinders are parallel to the surface, and the electric field which prefers that the cylinders be aligned with it, perpendicular to the substrate. If the system were semi-infinite, the intermediate phase would simply be labeled a surface phase, one of different symmetry than that of the bulk, a very common situation⁷. Such a phase would be expected to persist in the case of a finite, thick film. However when the film is sufficiently thin, the clear distinction between bulk and surface properties can no longer be made, and the two orientations compete throughout the film, resulting in the elimination of one of them.

Most theoretical work on block-copolymers in electric fields has focused on lamellar-forming phases, as opposed to cylindrical ones, and on the dynamic mechanisms by which morphologies could realign, rather than on the equilibrium morphologies themselves. Such dynamic mechanisms were the subject of the seminal papers of Amundson et al.^{6,8}, and of more recent dynamic density functional calculations^{9,10,11}. The form of the equilibrium phases was taken up by Pereira and Williams¹² and by Tsori and Andelman¹³. Both groups considered one intermediate phase in which a single lamella at the plates remains parallel to them, although surface fields could conceivably lead to a sequence of intermediate phases distinguished by the number of lamellae parallel to the surface. Such a discrete increase, or decrease, of the number of lamellae with applied field would be analogous to the layer-by-layer growth modes observed in adsorbed films¹⁴. Both groups presented phase diagrams as functions of applied electric field and film thickness. Although similar, they differ in one respect: that of Tsori and Andelman shows the perpendicular phase to be favored always at sufficiently large external fields, which is certainly correct. The effects of surface fields have also been explored^{10,11,13}. As expected, a strong surface field favors the formation of an intermediate phase. The evolution of morphology with external field in a single lamella has recently been studied by Matsen using self-consistent field theory¹⁵.

As for cylindrical-forming diblocks in an external electric field, the only published work has again focused on the mechanisms of morphology realignment. This has been studied

experimentally¹⁶, and also theoretically by dynamical self-consistent field theory^{11,16}. The advantage of this technique is that one follows the dynamics of the system, and one can clearly see how different are the pathways towards an equilibrium morphology depending upon the initial configuration. The actual equilibrium morphologies, which are the focus of our interest, are difficult to achieve however, just as they often are in experiment.

Some insight into the expected phase diagram of the cylinder-forming diblock copolymer system can be garnered from the behavior of the lamellar-forming ones. In both systems, surface fields prefer an orientation which is different from that preferred by the electric field. It should be noted that this holds irrespective of whether the surface fields prefer one monomer species, A , or the other, B . Thus we should expect to obtain a phase of cylinders parallel to the surface when the electric field is weak, a phase of perpendicular cylinders when the electric field is strong, and an intermediate phase for thick films, and ones subject to large surface fields. The principal difference between the cylinder- and lamellar-forming systems will be in the symmetry of the surface phase. Similarly the principle difference between cylinder-formers adsorbed on a substrate that prefers the minority monomer, A , and those adsorbed on a surface preferring the majority monomer, B , will be in the specific morphology of the surface phase. Otherwise the general form of the phase diagrams of these systems is expected to be similar due to the identity of the underlying physics.

In this paper, we study a cylinder-forming block-copolymer system in external electric fields and examine the morphology and phase behavior in the presence of surface fields which prefer the minority monomer. In section II, we first show that some general features of the surface phase diagram in the electric field-chemical potential plane are easily discerned from basic thermodynamics, and without detailed calculation. However thermodynamics does not tell us the nature of the intermediate phases, while specific calculation does. We then turn to self-consistent field theory, and solve exactly the self-consistent equations and the Maxwell equations in the manner used by us previously for a bulk phase¹⁷. Subsequently, the same idea has been employed with a different technical implementation in other systems^{15,18}. As a consequence of solving the Maxwell equations exactly, we do not assume, as in refs.^{10,11,16}, that the effect of the electric field is weak; that is, that the fractional variation of the dielectric constant throughout the morphology is small¹⁹. Our results are presented in section III. For weak surface fields, or thin films, there is no intermediate phase, and we find the first of the scenarios suggested by Thurn-Albrecht et al⁴. The phase of parallel cylinders transforms

directly to one of perpendicular cylinders. These cylinders are, of course, affected in their structure by the presence of the substrate surface fields, but a cross-section parallel to the substrate confirms the hexagonal order, even very close to the substrate.

For stronger surface fields or thicker films, we find an intermediate phase in which a layer adjacent to the plates has a different morphology than that of the field-aligned cylinders in the rest of the film. The morphology is not one of cylinders parallel to the plates, but has the same hexagonal symmetry as a cross-section of the field-aligned aligned cylinders. However the distribution of monomers is altered so that the monomer favored by the surface field occupies a larger surface area than it would had the cylinders extended to the surface.

We conclude with a brief discussion and comparison of our results with experiment. In particular we find, in agreement with experiment in the presence of strong surface fields, that the phase boundary between the perpendicular phase and the intermediate phase is a weak function of film thickness for large thicknesses. Along this locus of first order transitions, the perpendicular and intermediate phases coexist. However as we just noted, the boundary layer of the intermediate phase does not consist of cylinders parallel to the substrate. Thus parallel cylinders do not exist in either phase, and one would not observe *in equilibrium*, along this particular phase boundary, the coexistence of cylinders in both parallel and perpendicular orientations.

II. THEORY

A. Thermodynamics

Because we are dealing with a surface film, we consider the excess free energy per unit area, or surface free energy per unit area, σ , defined as follows. Let F_{tot} be the total free energy of the system of volume $\Omega = d_0\mathcal{A}$ such that the free energy per unit volume,

$$f_b \equiv \lim_{\Omega \rightarrow \infty} \frac{F_{tot}}{\Omega}, \quad (1)$$

is the Legendre transform of the energy per unit volume, e_b , with respect to the entropy density, s_b , number density, ρ_b , and displacement field i.e.

$$f_b = e_b - s_b T - \rho_b \mu - \mathbf{D}_b \cdot \mathbf{E}, \quad (2)$$

with \mathbf{D}_b and \mathbf{E} the volume-averaged displacement and electric fields. Then the excess free energy per unit area, σ , is

$$\sigma \equiv \lim_{\mathcal{A} \rightarrow \infty} \frac{F_{tot} - f_b \Omega}{\mathcal{A}} \quad (3)$$

with the differential

$$d\sigma = -s_s dT - \rho_s d\mu - D_s dE_{ext}. \quad (4)$$

Here s_s is the excess entropy per unit area, ρ_s the excess number of particles per unit area, and E_{ext} is the externally applied field which is equal to the spatially averaged electric field¹⁷. The quantity D_s is the magnitude of the *surface contribution* to the displacement field, or surface excess displacement field

$$\mathbf{D}_s \equiv \lim_{\mathcal{A} \rightarrow \infty} \frac{1}{\mathcal{A}} \int [\mathbf{D}(\mathbf{r}) - \mathbf{D}_b(\mathbf{r})] d^3r, \quad (5)$$

where $\mathbf{D}_b(\mathbf{r})$ is the displacement field in the bulk cylindrical phase. The surface excess displacement field is in the x direction, normal to the plates.

From this differential, one easily finds a Clausius-Clapeyron equation pertaining to the surface phases. If one plots the phase diagram at fixed temperature in the electric field-chemical potential plane, then the slope of the boundary between surface phases, $dE_{ext}/d\mu$, is given by

$$\frac{dE_{ext}}{d\mu} = -\frac{\Delta\rho_s}{\Delta D_s}, \quad (6)$$

where $\Delta\rho_s$ and ΔD_s are the differences in the excess surface densities and displacement fields in the two phases. At zero external field, there are an infinite number of parallel phases distinguished by the integer number of layers of cylinders, and a perpendicular phase in which the cylinders are perpendicular to the substrate. The transitions between all phases are generally first-order; those between the perpendicular and parallel phases are first-order due to the difference in symmetry between them; those between different parallel phases are generally first order because an additional layer of parallel cylinders cannot be added in a continuous manner. As one turns on the electric field, the phase space of the perpendicular phase will increase, and that of the parallel phases will decrease. It is clear that the spatially averaged polarization will be smaller in the parallel phases than in the perpendicular phase, and so the displacement field will decrease discontinuously on entering a parallel phase from a perpendicular phase, and will increase discontinuously when leaving a parallel phase. Further, the surface density is presumably a monotonically increasing function of the chemical

potential. Hence we expect from eq. 6 to find the infinite number of parallel phases to be enclosed by phase boundaries which, if no other phases are encountered, will be in the shape of wickets. The legs of each wicket meet the $E_{ext} = 0$ axis perpendicularly, because $\Delta D_s = 0$ in the absence of a field. The top of each wicket is locally horizontal, and the field at which it occurs defines the critical voltage at which that parallel phase disappears. In the region of phase space in which an intermediate phase appears, the Claussius-Clapeyron equation can be applied to the phase boundaries between it and the parallel phases, and between it and the perpendicular phase to obtain useful information relating the surface densities and displacement fields in the coexisting phases. It can also be applied, of course, to the lamellar-forming systems^{12,13}.

Another useful result,

$$D_s = -\frac{\partial\sigma}{\partial E_{ext}}, \quad (7)$$

follows from the differential eq. 4. We note that, whereas that component of the bulk, spatially averaged, displacement which is along the direction of the external field must be positive²⁰, that same component of the excess surface displacement need *not* be. In fact, as we expect that the presence of the surface can only disrupt the perfect alignment of the cylinders with the electric field, at least near the surfaces, we anticipate that D_s will be *negative*. It follows from eq. 7 that the excess free energy per unit area will *increase* with increasing electric field. This contrasts with the behavior of the *total* free energy, F_{tot} , and free energy per unit volume, f_b , which *decrease* with increasing external field.

B. Self-Consistent Field Theory

The method we employ has been described previously¹⁷ for a bulk system, and simply needs known modifications for the case of a surface film²¹. Thus its presentation here can be brief. We consider a melt of n A-B diblock copolymer chains, each of polymerization index $N = N_A + N_B$. The mole fraction of the A-monomers, $f_A = N_A/N$. We also assume that the Kuhn lengths of the A and B components are identical, a length denoted a . The system is confined between identical plates, a distance d_0 apart, each of area \mathcal{A} , which exert a surface field, $h(\mathbf{r})$, preferentially on one block with respect to the other. The plates are normal to the x axis, and the applied field is along the positive direction. The fraction of the volume occupied by polymer is denoted $\Phi_0(\mathbf{r})$, and is unity in the film except near the

plates where it falls to zero.

Self-consistent field theory leads to a free energy, F , which is a functional of unknown fields, W_A , W_B , Ξ , and the unknown electric potential, $V(\mathbf{r})$, and a function of temperature, T , volume, Ω , and area, \mathcal{A} . In an ensemble in which the external electric potential, V_0 , is held fixed²⁰, the free energy can be written

$$\begin{aligned} \frac{\mathcal{F}(W_A, W_B, \Xi, V; T, \Omega, \mathcal{A})}{nk_B T} &= -\ln \mathcal{Q}[W_A, W_B] \\ &+ \frac{1}{\Omega} \int d\mathbf{r} \{ \chi N \Phi_A \Phi_B - W_A \Phi_A - W_B \Phi_B \\ &- h(\mathbf{r}) N (\Phi_A - \Phi_B) - \Xi (\Phi_0 - \Phi_A - \Phi_B) \\ &- \frac{\Omega \epsilon_0 \kappa(\mathbf{r})}{2nk_B T} (\nabla V(\mathbf{r}))^2 \} , \end{aligned} \quad (8)$$

where ϵ_0 is the vacuum permittivity, k_B is Boltzmann's constant, and $\Phi_A(\mathbf{r})$ and $\Phi_B(\mathbf{r})$ are the local volume fractions of A and B monomers. The function $\mathcal{Q}[W_A, W_B]$ is the partition function of a single polymer chain subject to the fields $W_A(\mathbf{r})$ and $W_B(\mathbf{r})$, as is given below. The field $\Xi(\mathbf{r})$ is a Lagrange multiplier that enforces locally the incompressibility constraint, $\Phi_A(\mathbf{r}) + \Phi_B(\mathbf{r}) = \Phi_0$. The dependence on temperature, T , comes from the usual Flory interaction parameter, χ , which to a good approximation is inversely proportional to T . Finally the local dielectric constant is $\kappa(\mathbf{r})$. A constitutive relation between this local dielectric constant and the local volume fractions, $\Phi_A(\mathbf{r})$ and $\Phi_B(\mathbf{r})$, must be specified. We have chosen, as previously¹⁷, that the local dielectric constant be given by its local average. Here that choice is expressed

$$\kappa(\mathbf{r}) = \Phi_0 [\kappa_A \Phi_A(\mathbf{r}) + \kappa_B \Phi_B(\mathbf{r})] + 1 - \Phi_0, \quad (9)$$

where κ_A and κ_B are the dielectric constants of the pure A and B homopolymer phases respectively. Note that near the plates, the dielectric constant approaches unity. We stress that, while this choice is clearly correct in the limiting cases of the pure systems and in the weak segregation limit, it is simply a *choice*. While there are theories of the constitutive relation appropriate for dilute gases and for critical fluids, little is known of the detailed relation for dense, solid, multi-component systems. Hence that of eq. 9, which has the virtue of being both reasonable and simple, has been commonly employed^{10,11,15,16,17,18}.

The requirement that the free energy functional be an extremum with respect to variation of the electric potential, $V(\mathbf{r})$, $W_A(\mathbf{r})$, $W_B(\mathbf{r})$, $\Xi(\mathbf{r})$, and of the volume fractions $\Phi_A(\mathbf{r})$ and

$\Phi_B(\mathbf{r})$ at constant temperature, or χN , leads to the following set of equations:

$$0 = \nabla \cdot [\epsilon_0 \kappa(\mathbf{r}) \nabla V(\mathbf{r})] , \quad (10)$$

$$w_A(\mathbf{r}) = \chi N \phi_B(\mathbf{r}) + \xi(\mathbf{r}) - h(\mathbf{r}) N - \frac{\Omega \epsilon_0}{2nk_B T} \Phi_0(\mathbf{r}) \kappa_A (\nabla V(\mathbf{r}))^2 , \quad (11)$$

$$w_B(\mathbf{r}) = \chi N \phi_A(\mathbf{r}) + \xi(\mathbf{r}) + h(\mathbf{r}) N - \frac{\Omega \epsilon_0}{2nk_B T} \Phi_0(\mathbf{r}) \kappa_B (\nabla V(\mathbf{r}))^2 , \quad (12)$$

$$\Phi_0(\mathbf{r}) = \phi_A(\mathbf{r}) + \phi_B(\mathbf{r}) , \quad (13)$$

$$\phi_A(\mathbf{r}) = -\frac{\Omega}{\mathcal{Q}} \frac{\delta \mathcal{Q}}{\delta w_A(\mathbf{r})} , \quad (14)$$

$$\phi_B(\mathbf{r}) = -\frac{\Omega}{\mathcal{Q}} \frac{\delta \mathcal{Q}}{\delta w_B(\mathbf{r})} . \quad (15)$$

The functions W_A , W_B , Ξ , Φ_A and Φ_B , which satisfy these equations are denoted by lower case letters, w_A , w_B , ξ , ϕ_A , ϕ_B , respectively. The first of these equations is simply Gauss's law for a system with no free charge. The free energy within the self-consistent field approximation, F_{scf} , is obtained by substitution of these functions into the free energy of eq. (8),

$$F_{\text{scf}}(V_0, T, \Omega, \mathcal{A}) = \mathcal{F}(w_A, w_B, \xi, V; T, \Omega, \mathcal{A}) , \quad (16)$$

or

$$\frac{F_{\text{scf}}}{nk_B T} = -\ln \mathcal{Q}[w_A, w_B] - \frac{1}{\Omega} \int d\mathbf{r} \left\{ \chi N \phi_A(\mathbf{r}) \phi_B(\mathbf{r}) + \xi(\mathbf{r}) \Phi_0(\mathbf{r}) + \frac{\Omega \epsilon_0}{2nk_B T} [1 - \Phi_0(\mathbf{r})] [\nabla V(\mathbf{r})]^2 \right\} . \quad (17)$$

The nature of the particular system being described by self-consistent field theory is specified by the partition function of a representative member of the entities which comprise the system, in this case, block copolymers. Therefore $\mathcal{Q}[w_A, w_B] = \int d\mathbf{r} q(\mathbf{r}, 1)/k$, where $q(\mathbf{r}, s)$ satisfies the modified diffusion equation

$$\frac{\partial q}{\partial s} = \frac{1}{6} N a^2 \nabla^2 q - w_A(\mathbf{r}) q, \quad \text{if } 0 \leq s \leq f_A , \quad (18)$$

and

$$\frac{\partial q}{\partial s} = \frac{1}{6} N a^2 \nabla^2 q - w_B(\mathbf{r}) q, \quad \text{if } f_A < s \leq 1 , \quad (19)$$

with the initial condition $q(\mathbf{r}, 0) = 1$, and k is a volume of no consequence here.

The total density profile, $\Phi_0(\mathbf{r})$, and the surface field, $h(\mathbf{r})$, must still be specified. We follow ref.²¹ and choose

$$\Phi_0(\mathbf{r}) = \frac{1}{2} [1 - \cos(\pi x / \epsilon)], \quad 0 \leq x \leq \epsilon$$

$$\begin{aligned}
&= 1, & \epsilon \leq x \leq d_0 - \epsilon \\
&= \frac{1}{2}[1 - \cos(\pi(d_0 - x)/\epsilon)], & d_0 - \epsilon \leq x \leq d_0
\end{aligned} \tag{20}$$

and

$$\begin{aligned}
h(\mathbf{r}) &= \frac{\Lambda a N^{1/2}}{\epsilon} [1 + \cos(\pi x/\epsilon)], & 0 \leq x \leq \epsilon \\
&= 0, & \epsilon \leq x \leq d_0 - \epsilon, \\
&= \frac{\Lambda a N^{1/2}}{\epsilon} [1 + \cos(\pi(d_0 - x)/\epsilon)], & d_0 - \epsilon \leq x \leq d_0,
\end{aligned} \tag{21}$$

where ϵ is a small distance given below, and Λ is the strength of the surface field. A positive value of Λ causes the surface of the system to prefer the A component.

Because of the three-dimensional nature of the problem, we have chosen to solve the self-consistent equations in real-space, following the pseudo-spectral method of Rasmussen and co-workers^{22,23,24}. We have taken a grid which is $192 \times 32 \times 64$ in the x, y, z directions respectively. The length ϵ is chosen to be sufficiently small to ensure that it does not affect phase behavior. It is discussed further, below. In examining the phase of cylinders parallel to the plates, whose axes are in the z direction, we have investigated several arrangements of the cylinders, and varied the distances between them, both in the x and y directions, to ensure that we have found the minimum free energy configuration.

III. RESULTS

The parameter space of our system is large, as its state is specified by five variables, the choice of which is not unique. They are the temperature, or equivalently, χN , the applied electric field, E_{ext} , the chemical potential, μ , or the film thickness d_0 , the surface field strength, ΛN , and the copolymer architecture, f_A . In order to demonstrate the various morphologies, we have chosen to fix $\chi N = 18$, and the architecture at $f_A = 0.29$ which corresponds to the fraction of methyl methacrylate in the poly-(methyl methacrylate)(PMMA)/polystyrene(PS) diblocks used by Thurn-Albrecht et al.⁴. This leaves three parameters whose effects can be explored. We have chosen to vary E_{ext} and d_0 , and have examined two surface field strengths, $\Lambda N = 0.2$, and 0.5 . To understand whether these surface fields are weak or strong, the surface energy of n polymers subject to these fields, U_{su} , can be compared to the electrostatic field energy of these polymers in volume Ω . The

former of these energies is $U_{su} = nk_B T N \Lambda$, while in the bulk cylindrical phase, the latter is $U_{el} = \kappa_0 \epsilon_0 E_{ext}^2 \Omega / 2$, where

$$\kappa_0 = \kappa_A f_A + \kappa_B (1 - f_A), \quad (22)$$

is the average dielectric constant of the system. Thus we consider the ratio

$$\begin{aligned} \frac{U_{el}}{U_{su}} &= \frac{\epsilon_0 \kappa_0 E_{ext}^2 \Omega}{2 k_B T \Lambda N n}, \\ &= \frac{\kappa_0 E_{ext}^2}{2 \Lambda N \mathcal{E}^2}, \\ &= \frac{\kappa_0 \hat{E}_0^2}{2 \Lambda N}, \end{aligned} \quad (23)$$

where we have introduced the convenient scale of electric field

$$\mathcal{E} \equiv \left(\frac{k_B T n}{\epsilon_0 \Omega} \right)^{1/2}, \quad (24)$$

and the value of the external field in these units, $\hat{E}_0 \equiv E_{ext} / \mathcal{E}$. At typical temperatures, $T \approx 430K$, and for a typical volume per polymer chain of 100 nm^3 , this unit of electric field is $\mathcal{E} \approx 82V/\mu\text{m}$. At experimental temperatures around 160°C the dielectric constants appropriate to the PMMA-PS copolymer, with PMMA being the A block and PS the B block are^{4,25,26} $\kappa_A = 6.0$ and $\kappa_B = 2.5$, from which $\kappa_0 \approx 3.52$. Thus $U_{el}/U_{su} \approx 1.8 \hat{E}_0^2 / \Lambda N$. At external fields of order of tens of volts per micron, the surface field energies we consider are comparable to the electrostatic energies, and are therefore smaller than the rather large surface fields²⁷ of the experiments of Xu et al.¹⁶.

We first consider the system with surface fields of $\Lambda N = 0.5$. We have calculated, for a given thickness, d_0 , the excess free energies of various parallel, perpendicular, and intermediate phases. That with the lowest excess free energy is the equilibrium one. Rather than plot the excess free energy, σ , directly vs. applied field, we note from eq. 3 and the fact that the electrostatic contribution to the bulk free energy of the cylindrical phase is simply $-\epsilon_0 \kappa_0 E_{ext}^2 / 2$, that for determining the globally stable phase, we can equally well plot the dimensionless surface free energy

$$f_n(\hat{E}_0) \equiv \frac{F_{tot}}{nk_B T} + \frac{1}{2} \kappa_0 \hat{E}_0^2. \quad (25)$$

The derivative of this function with respect to the dimensionless external field \hat{E}_0 can be found from eq. 7 to be the negative of the dimensionless excess displacement field

$$\hat{D}_s \equiv \frac{D_s}{d_0 \epsilon_0 \mathcal{E}},$$

$$= -\frac{\partial f_n(\hat{E}_0)}{\partial \hat{E}_0}. \quad (26)$$

In fig 1. we show the excess free energy f_n for several phases as a function of the dimensionless external electric field for a thickness $d_0 = 7.5N^{1/2}a$. First we note, as anticipated, that the surface free energy increases with external field, indicating that the surface contribution to the displacement is, in fact, negative *i.e.* in the opposite direction of the applied field. Secondly, we see that at this thickness, the stable morphology at small external fields is one with five layers of cylinders parallel to the plates. As the field is increased, a first order transition occurs to a mixed state in which the surface contribution to the displacement field is less negative. At sufficiently large fields, there is a second transition to the state in which all cylinders are parallel to the external field. The excess displacement field is even less negative, but is not zero due to the distortion of the cylinders near the plates. By repeating such calculations as a function of thickness, we obtain the phase diagram shown in fig. 2. Because the film thickness is a smooth function of the chemical potential, this diagram reflects much of what was anticipated earlier in our discussion of the phase diagram as a function of electric field and chemical potential. Note that for films of sufficient thickness to accommodate more than two layers of parallel cylinders, the surface field is sufficiently strong to impose a surface ordered layer which results in the existence of an intermediate phase. At higher fields, this surface ordered layer becomes too costly, and disappears resulting in the perpendicular phase. As anticipated, the electric field which brings about this latter transition varies relatively weakly with film thickness. For sufficiently thin films, both orientations of cylinders, characteristic of the intermediate phase, cannot be maintained leading to the elimination of the intermediate phase.

In determining the phase boundary between the perpendicular and intermediate phases, and between the perpendicular and the cylindrical phase with two parallel layers, we have set the characteristic length, ϵ , of the surface field to a constant value $3N^{1/2}a/16$. It is not difficult to see from eqs. 20, 21 that if ϵ is to equal an integer number n of grid points, of which there are 192 in the x direction, then the thickness $d_0/N^{1/2}a$ must take the discrete values $36/n$. These discrete points are shown in fig. 2 where they are connected by a spline fit, shown dotted, to guide the eye. In contrast to the relatively smooth variation with thickness of the electric field at the transition from the perpendicular phase, that at the transition from the parallel phase varies rapidly with thickness. Hence the discrete values of

thickness imposed by a constant ϵ is restrictive. Further, the behavior of this critical field with thickness has already been anticipated from our discussion of the thermodynamics of the transition. For these transitions, therefore, we chose ϵ to be a constant fraction of film thickness, $\epsilon/d_0 = 1/32$. It is readily seen, again from eqs. 20, 21, that this choice permits the film thickness $d_0/N^{1/2}a$ to vary continuously. We have compared the two values of the critical fields obtained from these two different choices of ϵ at the discrete values of $d_0 = 36/n$ permitted by a constant ϵ , and found essentially no difference.

We next present density profiles of the various phases for a distance between plates of $d_0 = 7.5aN^{1/2}$. When the applied field is zero, the stable phase is that shown in fig. 3 which we denote as having five parallel layers. The cut is in the x (vertical), y (horizontal) plane, a cut normal to the plane of the plates. The gray scale shows the volume fraction of A monomer from 0.0 (lightest) to 1.0 (darkest) in four bins of width 0.25. The A block is favored by the surface field of strength $\Lambda N = 0.5$. The distortion of the cylinders at the surface is clear. A cut in the yz plane, parallel to the plates, (not shown), confirms that these are, indeed cylinders with axis along the z direction.

With an applied field of sufficient strength, the intermediate state becomes globally stable. A cut in the xy plane is shown in fig. 4 for a value $\hat{E}_0 = 0.49$. Most of the film thickness is occupied by cylinders which are perpendicular to the plates, and a cut in the yz plane halfway between the plates, (not shown), confirms that the cylinders are in a hexagonal array. It might be expected from fig. 4 that, adjacent to the surface, one would find a distorted layer of cylinders, just as in fig. 3. That this is *not* the case is shown by a cut through the intermediate phase in a yz plane very near the surface, fig. 5. One sees instead that there is an *hexagonal* array, such that the surface-favored A monomers occupy most of the surface layer. Clearly the hexagonal arrangement on the surface derives from the hexagonal, perpendicular, arrangement of cylinders in most of the film. Comparison of a sequence of yz cuts confirm that the symmetry axes of the upright cylinders in this intermediate phase coincide with the symmetry axes of the hexagonal array at the surface; i.e. the A -rich cores of the cylinders stand directly above the B -rich centers of the surface pattern. That the A monomers near the surface are located *outside* of the cylinders thereby occupying a larger area in the unit cell is clearly an effect due to the surface field. Because the A monomers are the minority component, $f_A = 0.29$, this configuration cannot extend too far into the film.

For larger values of the electric field, the perpendicular phase is attained. Fig. 6 shows

the density profile in the xy plane at a field of $\hat{E}_0 = 0.78$. One clearly sees the distortion of the cylinders produced by the surface.

We next show, in fig. 7, the phase diagram for the weaker surface field of strength $\Lambda N = 0.2$. Again, we chose $\epsilon = 3N^{1/2}a/16$. One sees that the weaker surface field can no longer impose a surface morphology which differs from, yet coexists with, that of the remainder of the film, even for ones sufficiently thick to accommodate seven parallel layers. Thus there is no intermediate phase. Instead, with increasing external field, transitions from all cylindrical phases shown, up to seven parallel layers, are directly to the perpendicular phase. The maximum critical fields of the transition between parallel and perpendicular phases vary as $1/\sqrt{d_0}$, as expected. This behavior is shown in the inset. The six maximum critical fields are shown by the open triangles which fall on a straight line in this plot.

IV. DISCUSSION

We have applied self-consistent field theory to a planar film of cylindrical-forming block copolymers. The plates between which the film is adsorbed prefer the minority A component. In the absence of an electric field, this causes the morphology to be that of cylinders whose axes are parallel to that of the plates. We have studied the equilibrium phase diagram in the presence of an applied electric field which tends to align the cylinders perpendicular to the plates, and have solved the Maxwell equations without approximation. The behavior as a function of field and film thickness is, for the most part, similar to that of lamellar-forming diblocks. As argued above, this is because the underlying physics, that of the competition between bulk and surface phases, is the same. In particular for weak surface fields or thin films, the surface field cannot impose a surface morphology which differs from the rest of the film, so that there is no intermediate phase. The first-order transition with increasing electric field from the phase of parallel cylinders to that of perpendicular cylinders is direct. However for stronger surface fields and thicker films, an intermediate phase does appear, one which is characterized by a boundary layer near the plates.

The nature of this boundary layer is very different for cylinder-forming diblocks than for lamellar-forming ones for which this layer is simply a modulated lamellae. We considered different possibilities for this boundary layer. Because of the experimental report of a signal indicating the presence of both perpendicular and parallel cylinders⁴, we considered whether

a layer near the plates might consist of parallel cylinders, but found that it did not. In retrospect, this is not difficult to understand. First, the perpendicular cylinders aligned with the field could not connect in a simple periodic manner with cylinders aligned parallel to the plates as the two arrays would be incommensurate. Thus one of the two arrays would have to be distorted, with a concomitant increase of free energy. Second, the substrate does not favor parallel cylinders *per se*, rather it favors one monomer over the other, the minority A monomer in our case. In zero electric field, parallel cylinders are favored over perpendicular ones because the area of A monomers presented to the plates is larger in the former than in the latter. The ratio of areas is $\mathcal{A}_{par}/\mathcal{A}_{perp} \approx 1/f_A^{1/2} > 1$. In a non-zero field which favors the intermediate phase, however, the area presented to the plates by parallel cylinders is less than that presented in the configuration of hexagonal symmetry which we obtained and which is shown in Fig. 5. In this case the ratio of areas is $\mathcal{A}_{par}/\mathcal{A}_{int} \approx f_A^{1/2}/(1 - f_A) < 1$. We also note that this particular pattern of the surface layer derives from the fact that the minority A component is favored by the surface. Were the B component favored, as is the case in the system of Xu et al.¹⁶, one would expect the minority core of the cylinders to extend all the way to the plates over a range of surface fields, something which could be technologically useful. Only for very strong fields would the plates be essentially covered by the majority B component which would require the interior of the cylinders containing the A component to be truncated near the surface. This observation is in agreement with the dynamic self-consistent field theory results as seen in Fig. 11(b) of Xu et al.¹⁶ and Fig. 5 of Lyakhova et al.¹¹.

We have found a transition from the intermediate phase to the perpendicular phase for which the electric field needed to bring about the transition varies only weakly with film thickness. It would seem that this could be identified with the transition observed by Thurn-Albrecht et al.⁴. There are, however, two difficulties with this interpretation. The first is that the electric field values at the transition are, in our calculation, larger than those observed in experiment. Further, the strength of the surface field in our calculation is weaker than that estimated in experiment. Were we to calculate critical electric fields for the stronger substrate fields of experiment, we would obtain even larger values as the critical electric field is expected to increase as the square root of the surface field. This comparison is reminiscent of that between calculated^{15,17} and experimental²⁵ electric field values for the transition from a body-centered cubic phase to a cylindrical phase in which the former were

also much larger than the latter. Explanations for this have been proposed^{18,26} which may resolve this difficulty. Even so, there remains the fact that, in the calculated intermediate phase, there are no cylinders in the parallel orientation. Therefore one would not observe *in equilibrium* the existence of both parallel and perpendicular cylinders along the phase coexistence of the intermediate and perpendicular phases. The resolution of this difficulty may be that, as the system cools from the disordered into the ordered phase, cylinders are nucleated near the plates in a configuration parallel to them while the major part of the film nucleates cylinders aligned with the electric field. Rearrangement of cylinders near the plates into that boundary layer which we predict to be the equilibrium one would presumably be a very slow process. If the boundary layer did not attain its equilibrium configuration, the experimental signal which detects both orientations of cylinders could be understood.

We thank K. Ø. Rasmussen for helpful correspondence, and D. A. Andelman for seminal conversations. This work was supported by the U.S.-Israel Binational Science Foundation (B.S.F.) under grant No. 287/02 and the National Science Foundation under grant No. DMR-0503752.

-
- ¹ T. L. Morkved, M. Lu, A. M. Urbas, E. E. Ehrichs, H. M. Jaeger, P. Mansky, and T. P. Russell, *Science* **273**, 931 (1996).
 - ² M. Park, C. Harrison, P. M. Chaikin, R. A. Register, and D. H. Adamson, *Science* **276**, 1401 (1997).
 - ³ S. Walheim, E. Schaffer, J. Mlynek, and U. Steiner, *Science* **283**, 520 (1999).
 - ⁴ T. Thurn-Albrecht, J. DeRouchey, and T. P. Russell, *Macromolecules* **33**, 3250 (2000).
 - ⁵ T. Thurn-Albrecht, J. Schotter, G. A. Kastle, N. Emley, T. Shibauchi, L. Krusin-Elbaum, K. Guarini, C. T. Black, M. T. Tuominen, and T. P. Russell, *Science* **290**, 2126 (2000).
 - ⁶ K. Amundson, E. Helfand, X. Quan, S. D. Hudson, and S. D. Smith, *Macromolecules* **27**, 6659 (1994).
 - ⁷ T. Arnold, R. K. Thomas, M. Castro, S. M. Clarke, L. Messe, and A. Inaba, *Phys. Chem. Chem. Phys.* **4**, 345 (2002).
 - ⁸ K. Amundson, E. Helfand, X. Quan, and S. D. Smith, *Macromolecules* **26**, 2698 (1993).
 - ⁹ A. V. Kyrylyuk, A. V. Zvelindovsky, G. J. A. Sevink, and J. G. E. M. Fraaije, *Macromolecules* **35**, 1473 (2002).
 - ¹⁰ K. S. Lyakhova, A. V. Zvelindovsky, and G. J. A. Sevink, *Slow Dynamics in Complex Systems*, M. Tokuyama and I. Oppenheim eds., Springer p. 217 (2004).
 - ¹¹ K. S. Lyakhova, A. V. Zvelindovsky, and G. J. A. Sevink, *Macromolecules* **39**, 3024 (2006).
 - ¹² G. G. Pereira and D. R. M. Williams, *Macromolecules* **32**, 8115 (1999).
 - ¹³ Y. Tsori and D. Andelman, *Macromolecules* **35**, 5161 (2002).
 - ¹⁴ R. Pandit, M. Schick, and M. Wortis, *Phys. Rev. B* **26**, 5112 (1982).
 - ¹⁵ M. W. Matsen, *Phys. Rev. Lett.* **95**, 2583021 (2005).
 - ¹⁶ T. Xu, A. V. Zvelindovsky, G. J. A. Sevink, K. S. Lyakhova, H. Jinnai, and T. P. Russell, *Macromolecules* **38**, 10788 (2005).
 - ¹⁷ C.-Y. Lin, M. Schick, and D. Andelman, *Macromolecules* **38**, 5766 (2005).
 - ¹⁸ M. W. Matsen, *J. Chem. Phys.* **124**, 0749061 (2006).
 - ¹⁹ Y. Tsori, D. Andelman, C.-Y. Lin, and M. Schick, *Macromolecules* **39**, 289 (2006).
 - ²⁰ L. D. Landau, E. M. Lifshitz, and L. P. Pitaevskii, *Electrodynamics of Continuous Media* (Pergamon Press, Oxford, 1984).

- ²¹ M. W. Matsen, *J. Chem. Phys.* **106**, 7781 (1997).
- ²² K. O. Rasmussen and G. Kalosakas, *J. of Polymer Sciences: Part B: Polymer Physics* **40**, 1777 (2002).
- ²³ G. Tzeremes, K. O. R. T. Lookman, and A. Saxena, *Phys. Rev. E* **65**, 041806 (2002).
- ²⁴ K. O. Rasmussen, *J. of Polymer Sciences: Part B: Polymer Physics* **42**, 3695 (2004).
- ²⁵ T. Xu, A. V. Zvelindovsky, G. J. A. Sevink, O. Gang, B. Ocko, Y. Zhu, S. P. Gido, and T. P. Russell, *Macromolecules* **37**, 6980 (2004).
- ²⁶ Y. Tsori, F. Tournilhac, D. Andelman, and L. Leibler, *Phys. Rev. Lett.* **90**, 145504 (2003).
- ²⁷ P. Mansky, Y. Liu, E. Huang, T. P. Russell, and C. Hawker, *Science* **275**, 1458 (1997).

V. FIGURE CAPTIONS

Fig. 1 Dimensionless excess surface free energy, f_n , eq. 25, as a function of applied field, \hat{E}_0 , for thickness $d_0 = 7.5N^{1/2}a$. The value of $\chi N = 18$, and the surface field is $\Lambda N = 0.5$. The free energy of the perpendicular phase is shown with a solid line, that of the intermediate phase with a dashed-dotted line, and that of the parallel phase of five layers is shown with a dotted line.

Fig. 2 Phase diagram as a function of electric field, \hat{E}_0 , and thickness, $d_0/N^{1/2}a$. The value of $\chi N = 18$, and the surface field is $\Lambda N = 0.5$. Parallel phases are denoted by a roman numeral corresponding to the number of cylinders in the film. The intermediate and perpendicular phases are marked “Intermed”, and “Perp” respectively. Discrete calculated points on the boundary between perpendicular and intermediate phases are shown by solid dots. The dotted line is a spline fit to them.

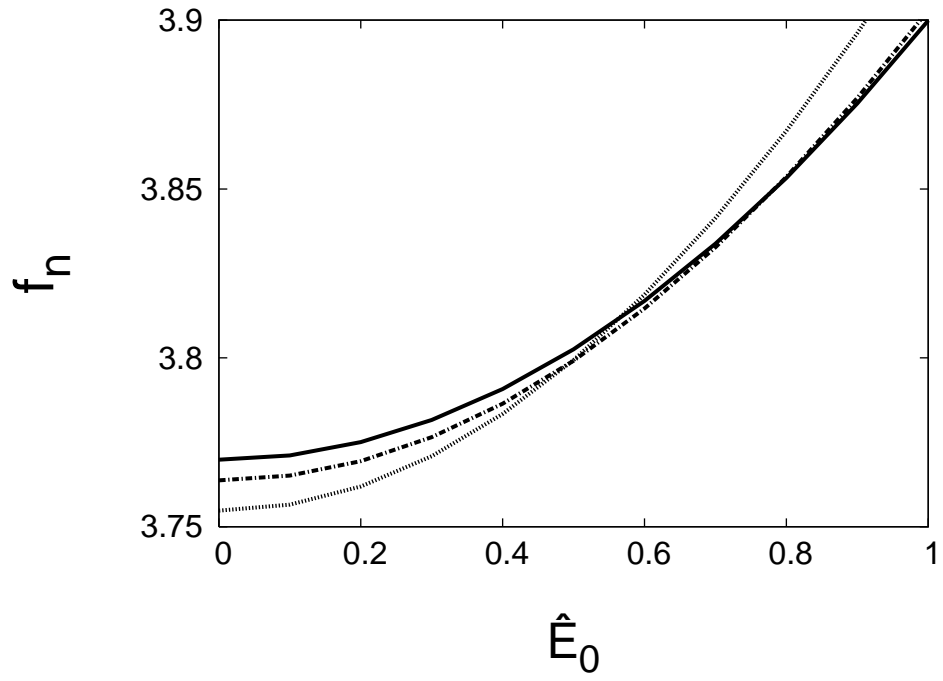
Fig. 3 Density profile in the xy plane of the parallel phase with five layers of cylinders. The thickness is $d_0/N^{1/2}a = 7.5$, and the applied field is zero. The gray scale shows the volume fraction of A monomer from 0.0 (lightest) to 1.0 (darkest) in four bins of width 0.25.

Fig. 4 Density profile in the xy plane of the intermediate phase. The thickness is $d_0/N^{1/2}a = 7.5$ and the applied field is now $\hat{E}_0 = 0.49$

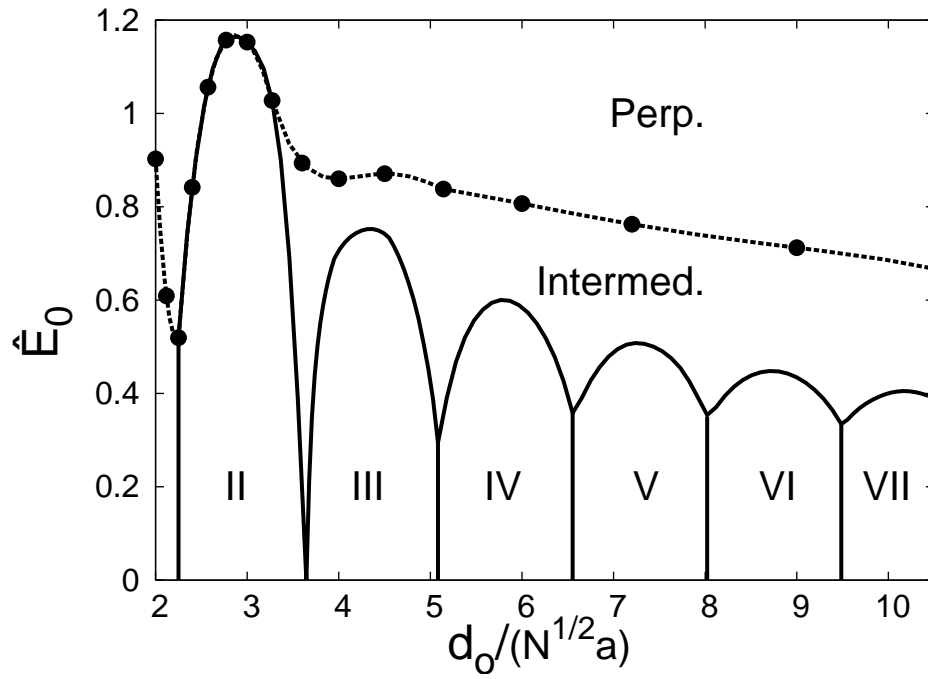
Fig. 5 Density profile of the intermediate phase shown here in a yz plane very close to the plates.

Fig. 6 Density profile of the perpendicular phase in the xy plane. The thickness is $d_0/N^{1/2}a = 7.5$ and the applied field is now $\hat{E}_0 = 0.78$

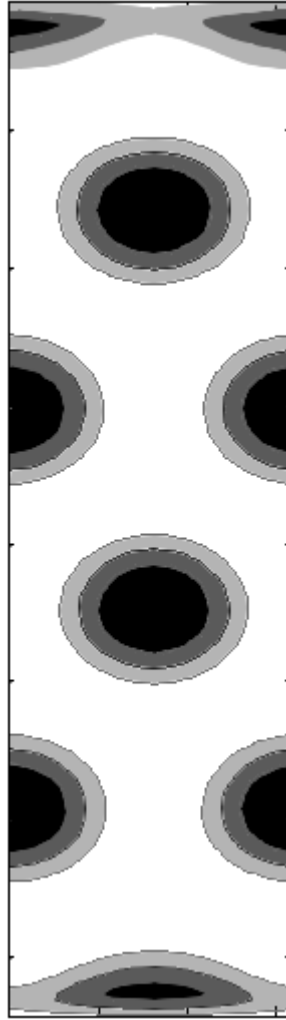
Fig. 7 Phase diagram as a function of electric field, \hat{E}_0 and thickness $d_0/N^{1/2}a$ for a surface field $\Lambda N = 0.2$ and $\chi N = 18$. Inset shows as open triangles six calculated maximum electric field values at the transition from parallel to perpendicular phases plotted vs. $1/d_0^{1/2}$.



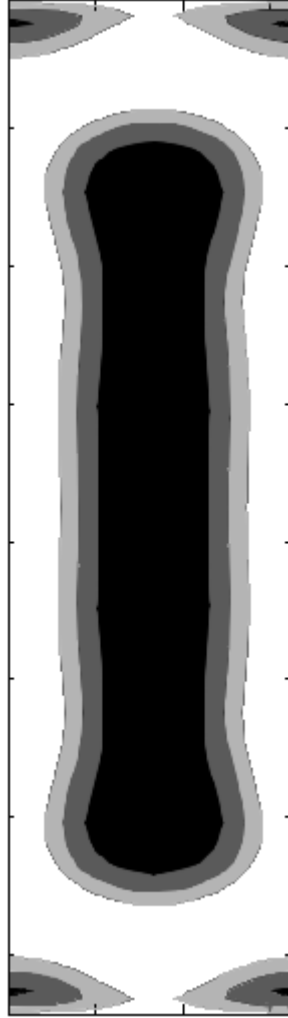
Chin-Yet Lin and M. Schick, Fig. 1



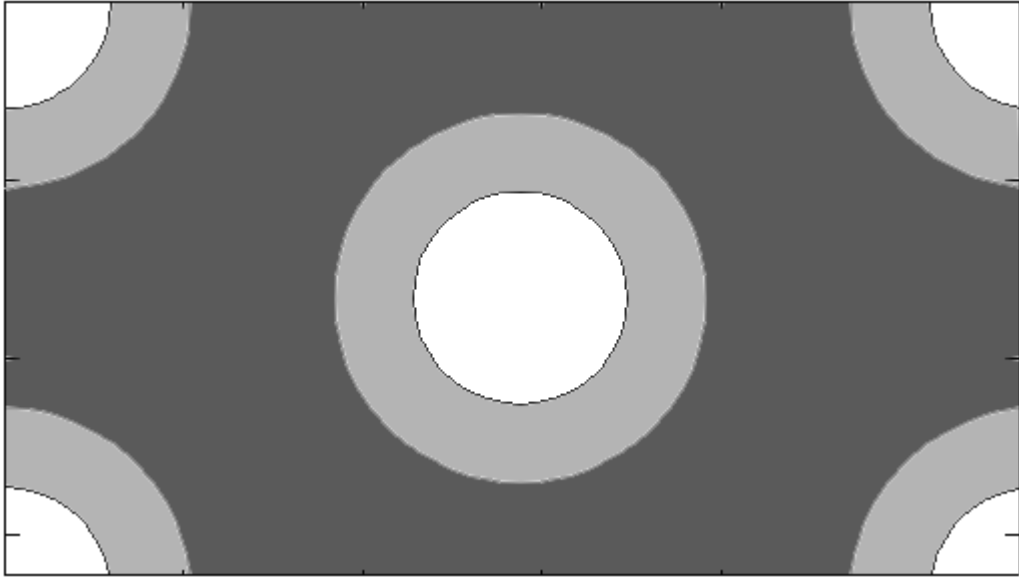
Chin-Yet Lin and M. Schick, Fig. 2



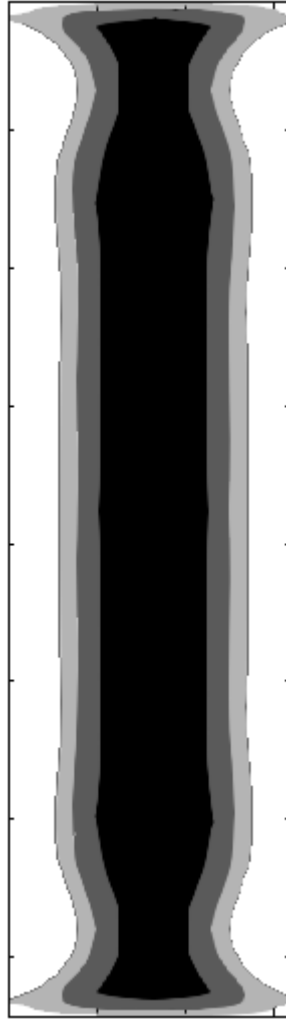
Chin-Yet Lin and M. Schick, Fig. 3



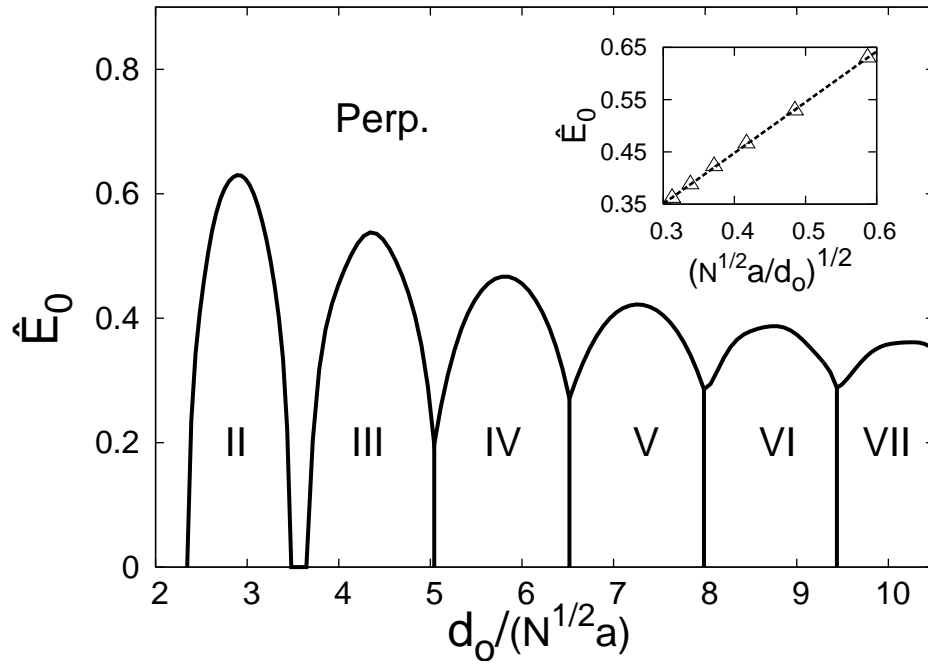
Chin-Yet Lin and M. Schick, Fig. 4



Chin-Yet Lin and M. Schick, Fig. 5



Chin-Yet Lin and M. Schick, Fig. 6



Chin-Yet Lin and M. Schick, Fig. 7